Estimation of Early Fatigue Damage in Heat Treated En-8 Grade Steel

P. Talukdar, S.K. Sen, and A.K. Ghosh

(Submitted 13 May 1996; in revised form 20 October 1997)

Generally, the failure of major machinery parts is due to fatigue damage. Because of the structural inhomogeneity of metals, fatigue damage may sometimes occur significantly below the yield strength of the material due to microplastic deformation at low stress levels. Commercial En-8 grade steel (widely used for making secondary metalworking products) was used to estimate the fatigue damage response during cyclic loading nearer to the fatigue endurance limit. Estimation of fatigue damage was carried out with the aid of a nondestructive testing (NDT) method, that is, Elastosonic measurement of fatigue damping coefficient and slope of fatigue damping curves. Results indicate that fatigue damage increases in annealed En-8 steel with an increase in peak stress and with an increase in the number of cycles. However, for hardened and tempered En-8 steel, experimental results may not provide a true indication of fatigue damage during fatigue loading nearer to the endurance limit, most likely due to the more homogeneous structure. Generally, fatigue failure occurs in this grade of steel due to microcrack generation in the cementite of the pearlite phase of annealed steel.

Keywords crack growth, fatigue, grade En-8 steel

1. Introduction

Measurement of internal damping is of great significance in investigating and evaluating the process of microplasticity as well as fatigue of metals or materials. The evaluation of energy scattering within metal frequently leads to direct evidence of microplasticity. In the process of measuring the dynamic hysteresis loop, measurement of internal damping is done in the region where it is dependent on the amount of the deformation amplitude, etc. The evaluation of energy losses during one cycle of stress under long-term loading characterizes the kinetics of accumulation of fatigue damage (Ref 1, 2).

Early fatigue damage may occur due to lattice imperfections in the crystal structure of metals. Studies of the fatigue damage response were carried out earlier by a number of researchers using different NDT methods that are related to structure-sensitive properties of metals such as ultrasonic measurement of sound velocity, measurement of eddy current loss, and measurement of electrical conductivity or magnetic permeability (Ref 3-5).

The present investigation attempted to study and evaluate fatigue damage rate with the aid of a modern NDT method, that is, Ultrasonic (frequency less than 30,000 Hz) technique in En-8 grade steel.

2. Experimental Methods

2.1 Test Materials

The chemical composition of commercial-grade En-8 steel is given in Table 1. The steel is received in the annealed condition.

P. Talukdar, NIFFT, Hatia, Ranchi-834003; **S.K. Sen,** RDCIS, SAIL, Hinoo, Ranchi-834002; and **A.K. Ghosh,** Jadavpur University, Calcutta-700032, India.

2.2 Heat Treatment

En-8 grade rods (13 mm diam) were heated to 880 °C for 1 h, followed by furnace cooling or quenching in oil, and tempering at 550 °C for 1 h. The mechanical properties of the steel after heat treatment are given in Table 2.

2.3 Sample Preparation

Heat treated steel rods (13 mm diam) were used for fatigue specimen preparation. The fatigue specimen (Fig. 1) was machined, and the gauge portion of it was polished with fine emery paper and 0.3 μm diamond paste.

2.4 Fatigue Test

Fatigue specimens (Fig. 1) were used for axial fatigue testing. A computer-controlled servo-hydraulic dynamic testing machine (MTS 810; MTS Systems Corporation, Minneapolis,

Table 1 Chemical composition of experimental plain-carbon En-8 steel

Element	Composition, %
C	0.38
Mn	0.78
Si	0.33
S	0.030
P	0.023

Table 2 Mechanical properties of experimental plain-carbon En-8 steel at 25 °C

Condition	UTS, MPa	Elongation, %	Hardness, HV	Fatigue strength, MPa
Annealed	650	25	150	260
Hardened and tempered	850	21	232	380

MN) was used to produce fatigue deformation in the push-pull mode. Load versus strain graphs were plotted for 1, 10, 100, 200, 500, 1000, and 10,000 cycles after testing at different stress amplitudes by keeping the R value constant (–1.0, $R = P_{max}/P_{min}$, where P_{max} = maximum load and P_{min} = minimum load). Typical hysteresis loop values (load versus strain) of one annealed steel specimen obtained during fatigue deformation in the push-pull mode for various cycles are shown in Fig. 2. The specimens were deformed for a certain number of cycles at a different load spectrum or at a certain load spectrum for a different number of cycles. After fatigue deformation, the heat treated specimens were tested in ultrasonic equipment (Model Elastosonic, Nirmachal Engineering, P, Ltd., Bangalore, India) to measure the damping coefficient.

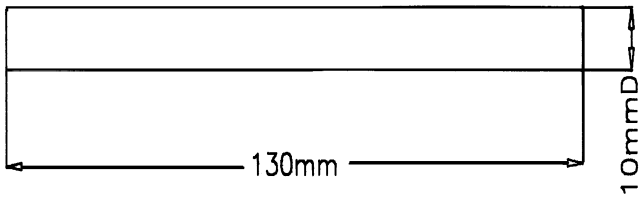

Fig. 1 Fatigue testing specimen

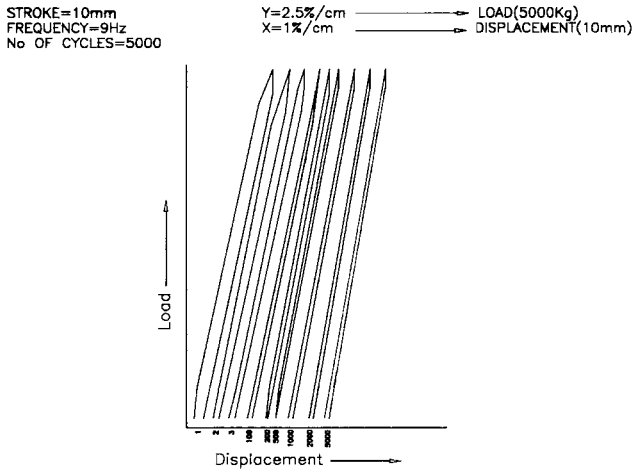

Fig. 2 Hysteresis loop (load versus displacement curve) of annealed steel for fatigue testing in the push-pull mode (specimen No. A2)

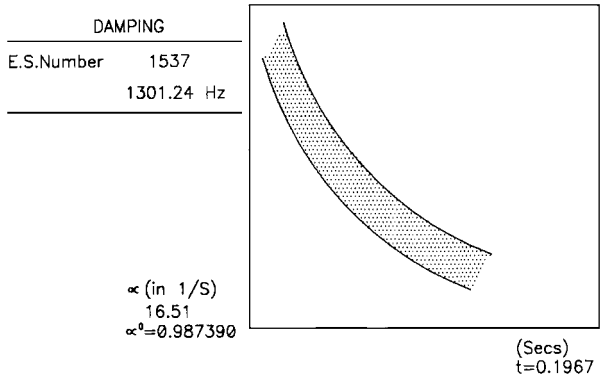

Fig. 3 Typical damping curve

3. Evaluation of Internal Damping of Fatigue Damaged Specimens

The data obtained from the computerized elastosonic equipment for the damping coefficient and the logarithmic decrement of cyclically deformed specimens are given in Tables 3 through 7 for various types of heat treatments. The experimental procedure used for evaluation of internal damping of fatigue specimens is as follows.

The test specimen was placed on the specimen holder so that the mid-zone of the specimen was positioned over the natural frequency sensor. The specimen was immediately tapped to obtain its natural frequency before the damping test. Damping data were obtained by tapping the fatigue deformed samples so as to obtain a smooth curve that was visible in the damping window.

The values of α (damping coefficient) and α_0 (logarithmic decrement of damping) corresponding to this curve were also displayed. A printout of the test results was also obtained. The computer program could be restarted for additional testing. A screen printout depicting the damping curve and a sample printout are shown in Fig. 3 and 4, respectively (Ref 6). Any material or body subjected to tapping experiences a slight dissipation of energy, which is vibrating exponentially in its fundamental frequency (Fig. 5). If the material undergoing testing has some internal defect, then that defect dampens the sound energy in the material very rapidly, thus resulting in significantly higher values. Mathematically,

$$\alpha_0 = e^{-\alpha T}$$

E.S. No. : 328 Frequency : 6097.56 Hz

Sl.No.	alpha	alpha-0	Sl.No.	alpha	alpha-0
1	19.70	0.99677	17	29.11	0.99524
2	12.98	0.99787	18	23.62	0.99613
3	14.19	0.99768	19	33.41	0.99454
4	16.37	0.99732	20	31.39	0.99486
5	19.91	0.99674	21	45.58	0.99255
6	18.19	0.99702	22	20.45	0.99665
7	23.68	0.99612	23	12.85	0.99790
8	26.89	0.99560	24	14.60	0.99761
9	33.20	0.99457	25	30.14	0.99507
10	36.71	0.99400	26	26.80	0.99562
11	31.47	0.99485	27	52.58	0.99141
12	40.65	0.99336	28	29.47	0.99518
13	36.47	0.99404	29	32.17	0.99474
14	39.68	0.99351	30	17.84	0.99708
15	35.05	0.99427	31	27.27	0.99554
16	31.80	0.99480	32	26.39	0.99568

STATISTICS

		alpha	alpha-0
No. of Tappings	:	32	-
Range (Minimum)	:	12.85	0.991415
Range (Maximum)	:	52.58	0.997896
Average	:	27.83	0.995447
Std. Deviation	:	9.55	0.001559

Fig. 4 Computer printout for specimen No. A1 annealed steel during damping coefficient measurement testing. (Peak stress, 275 MPa; stress amplitude, 37 MPa, 15,000 cycles

where T is the length of the cycle, α_0 is a dimensionless parameter, because it does not depend on the size and density of the material but on its integrity.

Hence, α_0 is a material intrinsic property. Values of α are reported in units of s^{-1}, where α is dependent on the integrity and dimensions of the material. The resultant cyclic deformation due to fatigue may be characterized as follows. If the value of α_0 for a material (for example, steel) of some dimensions decreases with respect to a constant value of α, this would indicate that damage during fatigue deformation increases due to cyclic loading (Ref 2, 3, 6).

Values of α and α_0 are shown on a damping curve or in a sample printout. The value of T can be obtained from the equation $\alpha_0 = e^{-\alpha T}$. For a constant value of α (for example, 45 s^{-1}), the value of α_0 is easily calculated for the same time period, T. Thus, α_0 was calculated for different fatigue cycles at a constant stress amplitude for a particular sample.

3.1 Discussion of Results

The graphs (Fig. 6 to 9) of logarithmic decrement of damping versus number of cycles and logarithmic decrement of damping versus peak stress were plotted from Tables 3 to 7. Figure 6, for example, indicates that α_o (logarithmic decrement of damping) for annealed steel decreases with an increase in the number of cycles for peak stresses of 275, 250, and 175 MPa. However, for a peak stress of 137 MPa after a certain number of cycles, the value of α_0 increases even though in all four cases the stress amplitudes were the same. At a comparatively higher peak stress (i.e., 275 MPa), the rate of decrease in the value of α_o with an increase in the number of cycles is much higher than for lower peak stresses (250 and 175 MPa).

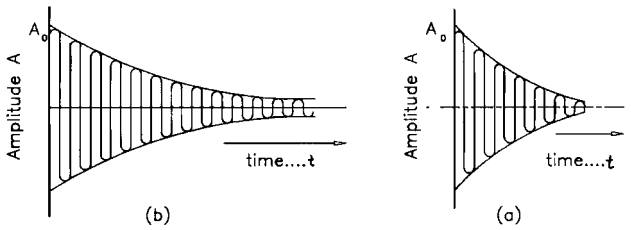

Fig. 5 Amplitude versus time curve for material dissipating energy; vibrates exponentially (a) without defects and (b) with defects

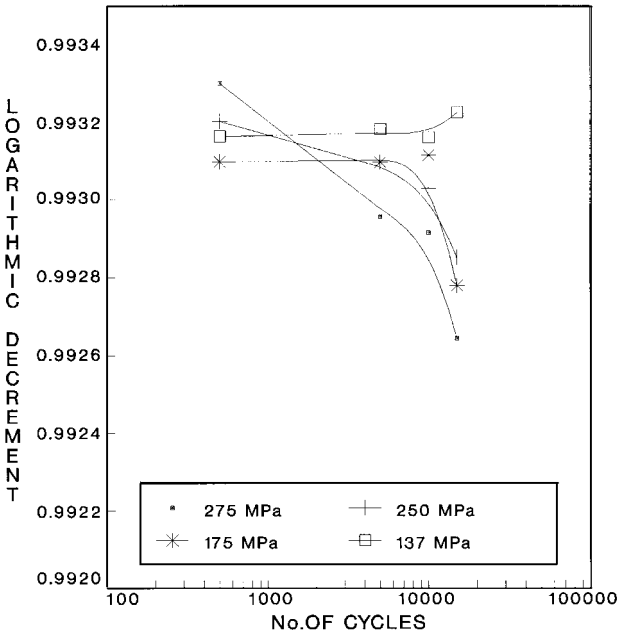

Fig. 6 Logarithmic decrement versus number of cycles for annealed steel

Table 3 Logarithmic decrement (α_0) versus No. of cycles for annealed steel

Specimen No.	Cycles, No.	α_0	Remarks
A1	500	0.993298	S_{max} = 275 MPa
	5,000	0.992956	S_a = 37 MPa
	10,000	0.992915	α = 45 s^{-1}
	15,000	0.992644	
A2	500	0.993201	S_{max} = 250 MPa
	5,000	0.993097	S_a = 37 MPa
	10,000	0.993030	α = 45 s^{-1}
	15,000	0.992852	
A3	500	0.993097	S_{max} = 175 MPa
	5,000	0.993096	S_a = 37 MPa
	10,000	0.993114	α = 45 s^{-1}
	15,000	0.992779	
A4	500	0.993162	S_{max} = 137 MPa
	5,000	0.993181	S_a = 37 MPa
	10,000	0.993159	α = 45 s^{-1}
	15,000	0.993223	
A5	500	0.993073	S_{max} = 112 MPa
	5,000	0.993137	S_a = 37 MPa
	10,000	0.993069	α = 45 s^{-1}
	15,000	0.993111	
A6	500	0.993223	S_{max} = 87 MPa
	5,000	0.993111	S_a = 37 MPa
	10,000	0.993071	α = 45 s^{-1}
	15,000	0.993229	

Note: S_{max}, peak stress; S_a, stress amplitude; α, damping coefficient

Table 4 Logarithmic decrement (α_0) versus No. of cycles for hardened and tempered (HT1) steel

Cycles, No.	α_o	Remarks
10	0.99435	S_{max} = 443 MPa
20	0.99415	S_a = 199 MPa
50	0.99432	α = 15 s^{-1}
100	0.99423	
200	0.99415	
500	0.99408	
1,000	0.99422	
2,000	0.99407	
5,000	0.99422	
10,000	0.99411	
12,000	0.99439	

Note: S_{max}, peak stress; S_a, stress amplitude; α, damping coefficient

The data indicate that for the higher peak stress of 250 MPa, the rate of decrease in α_0 is greater than that for the lower peak stress of 175 MPa. It may be concluded that α_0 decreases with an increase in the number of cycles and is greater for higher peak stress values. Similar trends were also observed in annealed steel (Fig. 7). Here, α_0 for annealed steel decreased more rapidly for 15×10^3 cycles than for 10×10^3 or 5×10^3 cycles with an increase in peak stress values. It was also shown that α_0 decreased more gradually for a comparatively higher number of cycles (i.e., 10, 5, and 15×10^3 cycles) because of the presence of a greater amount of fatigue damage.

Further analysis of Fig. 6 indicates that for up to a certain number of cycles there is practically no change in α_0 for annealed steel samples at lower fatigue peak stresses (175 and 137 MPa). It may thus be predicted that, for lower peak stress values of En-8 annealed steel, fatigue deformation up to a cer-

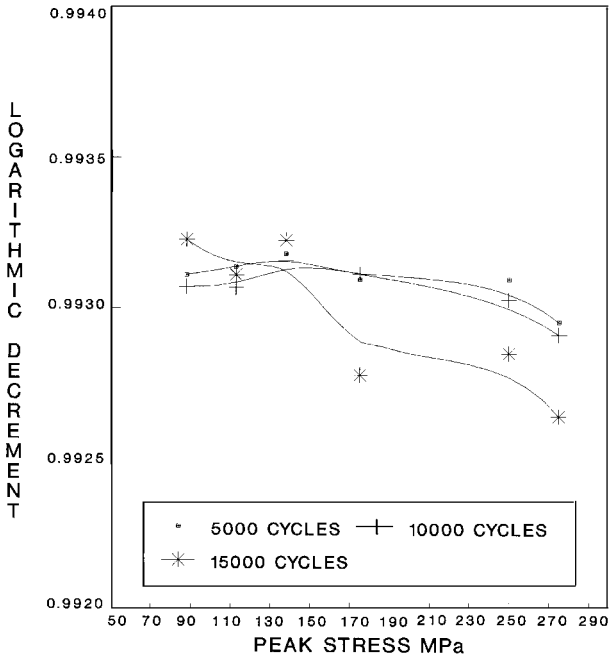

Fig. 7 Logarithmic decrement versus peak stress for annealed steel

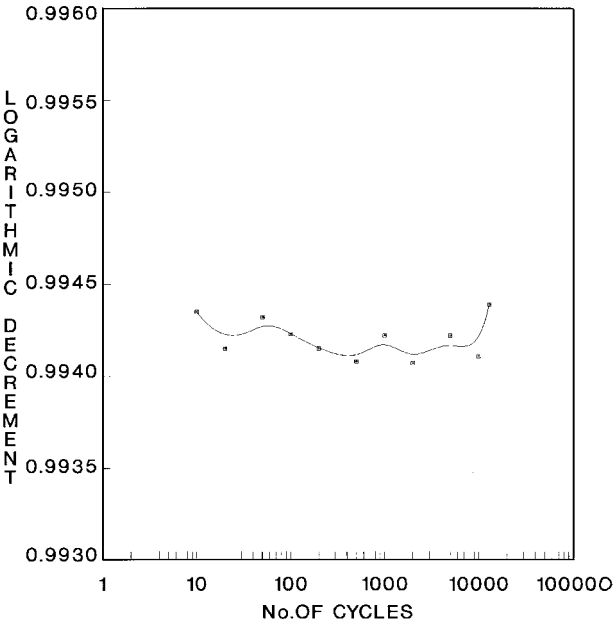

Fig. 8 Logarithmic decrement versus number of cycles for hardened and tempered steel

Table 5 Logarithmic decrement (α_0) versus peak stress for annealed steel

Specimen No.	Peak stress, MPa	α_0	Remarks
A1	275	0.992956	N = 5000
A2	250	0.993097	S_a = 37 MPa
A3	175	0.993096	$\alpha = 45\ s^{-1}$
A4	137	0.993181	
A5	112	0.993137	
A6	87	0.993111	
A1	275	0.992915	N = 10 000
A2	250	0.993030	S_a = 37 MPa
A3	175	0.993114	$\alpha = 45\ s^{-1}$
A4	137	0.993159	
A5	112	0.993069	
A6	87	0.993071	
A1	275	0.992644	N = 15 000
A2	250	0.992852	S_a = 37 MPa
A3	175	0.992779	$\alpha = 45\ s^{-1}$
A4	137	0.993227	
A5	112	0.993111	
A6	87	0.993229	

Note: N, no. of cycles; S_a, stress amplitude; α = damping coefficient

Table 6 Logarithmic decrement (α_0) versus peak stress for hardened and tempered steel

Specimen No.	Peak stress, MPa	α_0	Remarks
HT2	275	0.99773	N = 500
HT3	212	0.99772	S_a = 37 MPa
HT4	175	0.99770	$\alpha = 15\ s^{-1}$
HT5	137	0.99771	
HT6	112	0.99773	
HT7	87	0.99770	

Note: N, no. of cycles; S_a, stress amplitude; α, damping coefficient

Table 7 Logarithmic decrement (α_0) versus percentage of fatigue life for hardened and tempered steel

Specimen No.	Percentage of fatigue life	α_0	Remarks
HT8	10	0.993274	N_f = 24 000
HT9	20	0.988861	S_a = 125 MPa
HT10	50	0.983449	S_{max} = 600 MPa
HT11	80	0.981946	$\alpha = 45\ s^{-1}$

Note: N_f, no. of cycles to fatigue failure; S_a, stress amplitude; S_{max}, peak stress; α, damping coefficient

tain number of cycles is minimal and not detectable, because there is no change in α_0 values. After a higher number of cycles (5×10^3), the hysteresis loop (Fig. 2) decreases compared to a lower number of cycles (1, 2, or 3). This is due to a greater amount of fatigue softening in annealed steel.

The variations in logarithmic decrement of damping (α_0) for hardened and tempered En-8 steel with respect to the number of cycles or peak stresses are shown in Fig. 8 and 9, respectively. These graphs indicate that damage in metals cannot be predicted during this period of cyclic loading even when the peak stress is 443 MPa (stress amplitude 199 MPa) and the number of cycles is 12×10^3 even though this has been done previously in the case of annealed steel. The value of α_0 for annealed steel in Fig. 6 increases with an increase in the number of stress cycles (after certain number of cycles) even when the peak stress (137 MPa) is much lower than the endurance limit (260 MPa). Fatigue resistance, which thus may be increased during cyclic loading due to the amount of discontinuity with respect to crystal imperfection, may decrease in the annealed state (Ref 4, 7, 9).

Annealed En-8 steel consists of a ferrite-pearlite structure. During cyclic loading in the early stages of fatigue life, microplastic deformation may occur nearer to the endurance limit at the ferrite-pearlite grain boundary region. Therefore, after a certain number of cycles, the orientation of dislocations are as an array of slip bands, and subsequently, the annealed steel hardens. Finally, microcracks form in cementite phase in pearlite, and the value of α_0 for the steel may be decreased even further with an increase in the number of cycles (Fig. 6) (Ref 4, 7-9).

Variations in α_0 for hardened and tempered steel with respect to an increase in the number of cycles or peak stresses are shown in Fig. 8 and 9, thus illustrating the hardening and softening behavior of the steel. Hardened and tempered steel consists of a tempered martensite structure, which imparts toughness and strength to the steel, and the presence of discontinuities or point imperfections is lower compared to annealed steel. However, the presence of more lattice imperfections, that is dislocations, due to the presence of more retained austenite (more available grain boundary area for dislocations to accumulate) perhaps creates cyclic hardening and softening during the early stages of fatigue deformation (Ref 4, 9, 10).

Initially, with 10 to 20 cycles of loading, work hardening occurs, but subsequent cycling causes the rearrangement of dislocations, which offers less resistance to deformation. The material cyclically softens, and subsequently, the density of the dislocations rapidly increases with an increase in the number of loading cycles due to cyclic plastic straining and again causes significant cyclic strain hardening (Fig. 8).

With repeated cyclic hardening and softening, microcracks may initiate even at low stress for high cycles or in low cycles for higher stress conditions. Once fatigue cracking has initiated and propagated, the value of α_0 decreases somewhat with respect to the number of cycles (Fig. 10) (Ref 2, 4, 6, 7, 10). Fatigue cracking initiates either due to the cracking or debonding of the cementite in annealed steel (Ref 8). However, in hardened and tempered steel, it initiates in the martensite lath boundary or is segregated in the defect region (inclusion).

The logarithmic decrement with respect to the percentage of fatigue life is plotted in Fig. 10, which shows that α_0 decreases with advances in fatigue deformation or fatigue damage. The amount of fatigue damage as well as the remaining life of the metal after different loading cycles can be estimated using the present NDT technique.

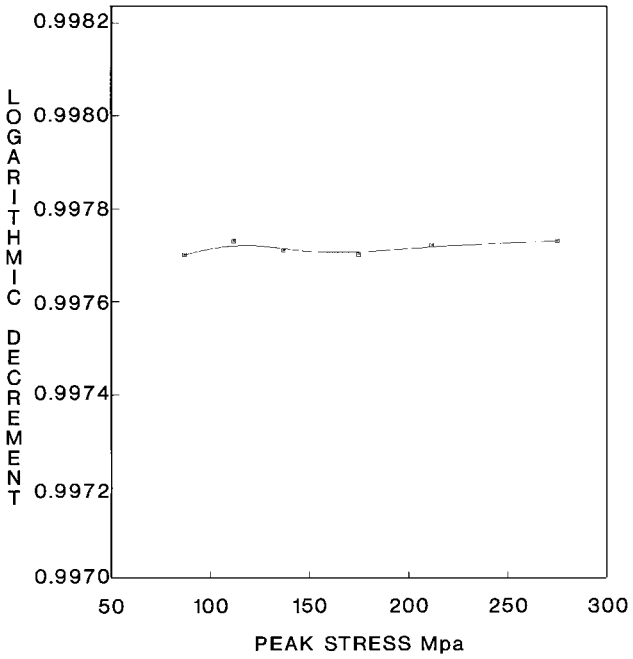

Fig. 9 Logarithmic decrement versus peak stress for hardened and tempered steel

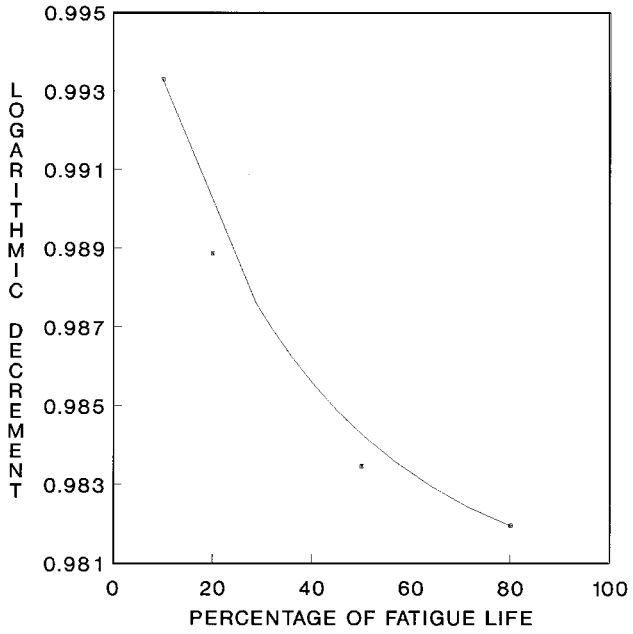

Fig. 10 Logarithmic decrement versus percentage of fatigue life for hardened and tempered steel

4. Conclusions

The rate of decrement of α_0 for annealed steel increases with an increase in the number of cycles at higher peak stress levels for constant stress amplitudes. The divergency of α_0 with respect to an increase in peak stress at constant stress amplitude for annealed steel is also greater for a greater number of cycles.

Fatigue damage is less when the peak stress of the loading spectrum is below the endurance limit. Fatigue resistance increases after a certain number of fatigue cycles when the peak stress is lower than the endurance limit, probably due to the decrease in crystal imperfections in annealed state.

The presence of lattice imperfections, that is, arrays of dislocations, in hardened and tempered En-8 steel perhaps creates cyclic hardening and softening during the early stages of fatigue deformation with peak stress nearer to the endurance limit.

Fatigue deformation progresses in the following manner: orientation of dislocations, formation of slip bands, and generation of microcracks in the cementite of the pearlite grains in annealed En-8 grade steel.

Resistance to fatigue deformation of annealed steel is less compared to hardened and tempered steel, because the amount of discontinuities with respect to point defects or crystal imperfections may be greater in the annealed state.

The fatigue life of heat treated En-8 steel may be measured using the calculated α_0 values obtained directly from a graph plotting the logarithmic decrement of damping (α_0) versus the percentage of fatigue life. Changes in the slope of the curve of logarithmic decrement of damping versus the number of cycles may be due to microcrack formation or the coalescence of microcracks during fatigue deformation.

References

1. A. Pusker and S.A. Golovin, Fatigue in Materials: Cumulative Damage Processes, *Mater. Sci. Monogr.*, No. 24, 1985, p 99-104
2. C.C. Smith, *Internal Friction and Ultrasonic Attenuation in Solids*, University of Manchester, Institute of Science and Technology, Manchester England, Pergamon Press, UK, 1980
3. *Proc. 3rd Europ. Conf.*, University of Manchester England, 18-20 July, 1980
4. G.E. Dieter, *Mechanical Metallurgy SI Metric Edition*, Mc-Graw Hill, London, 1988, p 375-438
5. A.K. Ghosh, T.K. Pal, and P. Talukdar, A Study of Low Stress Fatigue Damage of Welded Mild Steel, *IE(I) Journal-MM*, Vol 69, Mar 1989, p 65-69
6. *Manual of Elastosonic*, Nirmachal Engineering (P) Ltd., Bangalore, India, p 50-54
7. A. Pusker and S.A. Golovin, Fatigue in Materials: Cumulative Damage Processes, *Mater. Sci. Monogr.*, No. 24, 1985, p 145-165
8. S.K. Sen, D. Mukherjee, S. Mishra, and V. Ramaswamy, "An Evaluation of the Fatigue Performance of BOF Concast Rail Steel," *Proc. 5th Int. Conf. on Fatigue and Fatigue Thresholds*, FATIGUE'93, Montreal, Quebec, Canada, 3-7 May 1993
9. R.E. Reed-Hill, *Physical Metallurgy Principles*, 2nd ed., Affiliated East-West Press (P) Ltd., New Delhi, 1973, p 190-263
10. J.A. Bannantine, J.J. Comer, and J.L. Handrock, *Fundamentals of Metal Fatigue Analysis*, Prentice Hall, 1990, p 40-55
11. P. Talukdar, S.K. Sen, and A.K. Ghosh, "Estimation of Fatigue Damage in Annealed En-8 Grade Steel," National Seminar on Advances in the Manufacturing and Processing Technology of Alloy & Special Steels (AMPT-95), published in the proceedings, IIM, Ranchi, India, 21-22 Sept 1995, p 311-326